Coupling between Switching Regulation and Torque Generation in Bacterial Flagellar Motor

Fan Bai,[1,2] Tohru Minamino,[2] Zhanghan Wu,[3] Keiichi Namba,[2,*] and Jianhua Xing[3,†]

[1]*Biodynamic Optical Imaging Centre, Peking University, Beijing 100871, People's Republic of China*
[2]*Graduate School of Frontier Biosciences, Osaka University, 1-3 Yamadaoka, Suita, Osaka 565-0871, Japan*
[3]*Department of Biological Sciences, Virginia Tech, Blacksburg, Virginia, 24061-0406, USA*

The bacterial flagellar motor plays a crucial role in both bacterial locomotion and chemotaxis. Recent experiments reveal that the switching dynamics of the motor depend on the rotation speed of the motor, and thus the motor torque, nonmonotonically. Here we present a unified mathematical model which treats motor torque generation based on experimental torque-speed curves and the torque-dependent switching based on the conformational spread model. The model successfully reproduces the observed switching rate as a function of the rotation speed, and provides a generic physical explanation independent of most details. A stator affects the switching dynamics through two mechanisms: accelerating the conformational flipping rate of individual rotor-switching units, which contributes most when the stator works at a high torque and thus a low speed; and influencing a larger number of rotor-switching units within unit time, whose contribution is the greatest when the motor rotates at a high speed. Consequently, the switching rate shows a maximum at intermediate speed, where the above two mechanisms find an optimal output. The load-switching relation may serve as a mechanism for sensing the physical environment, similar to the chemotaxis mechanism for sensing the chemical environment. It may also coordinate the switch dynamics of motors within the same cell.

Many bacteria are propelled by several helical flagellar filaments, each driven at its base on the cell membrane by a bacterial flagellar motor (BFM). Using the transmembrane electrochemical proton (or sodium) motive force to power BFM rotation, free-swimming bacteria can propel their cell bodies at a speed of 15–100 μm/s, or up to 100 cell body lengths per second [1,2]. Flagellum rotation is one of the three main mechanisms for bacterial motility. The study of BFM has received high attention, with several decades of continuous efforts aimed at elucidating its functional mechanism and structural basis, and on finding applications in bionanotechnology.

Figure 1(a) gives a schematic top view of a BFM. A circular array of 8-11 stator complexes, anchored to the peptidoglycan, is located around the periphery of the rotor complex, which consists of ~26 identical units. In the extracellular part of the cell, a long flagellar filament (about 5 to 10 times the length of the cell body) is connected to the rotor. Protons flow from the periplasm to the cytoplasm through proton channels on the stator complex, driving a conformational change in the cytoplasmic domain of the stator complex, which in turn pushes the rotor to generate torque.

A BFM can stochastically switch its rotation between clockwise (CW) and counterclockwise (CCW) directions. When most of the motors on the membrane spin CCW, the flagellar filaments form a bundle and propel the cell steadily forward. When only a few motors (can be as few as one) spin CW, the flagellar filaments fly apart and the cell tumbles. Therefore, the cell repeats a run-tumble-run

pattern to perform a biased random walk. Regulation of the pattern is part of the well-studied chemotaxis system. External signals such as chemical attractants and repellents, temperature, and pH govern the concentration of the phosphorylated form of a signalling protein CheY, with CheY-P binding to the rotor biasing to CW rotation. Berg and coinvestigators further show that the motor can respond to mechanical signals as well [3,4]. An *E. coli* BFM first increases then decreases its switching rate upon the lowering of the mechanical load on its motor, with a maximum at around rotation speed of 100–150 Hz. It is intriguing that the motor integrates both chemical and mechanical signals and responds accordingly.

Various mathematical models have been proposed to explain the torque-generation and switching mechanisms of the BFM [5–10]. All these existing model studies treat the switching and torque-generation processes as two separate issues. The observation of Berg and coinvestigators indicates the necessity of a unified model. In this work, we present such a model to reveal how coupling between the two processes explains their observation. The model generalizes following aspects of the Ising-type conformational spread model proposed by Bray and Duke [5]:

(1) Each of the 26 identical rotor-switching units (RSUs) of the switch complex can be in one of four states, indicating whether it is bound (B) or not bound (b) by a CheY-P molecule, and whether it is in active (A, CW rotation) or inactive (a, CCW rotation) conformation [11]. Figure 1(b) presents a free-energy diagram of the four states of an individual RSU and the transitions among them.
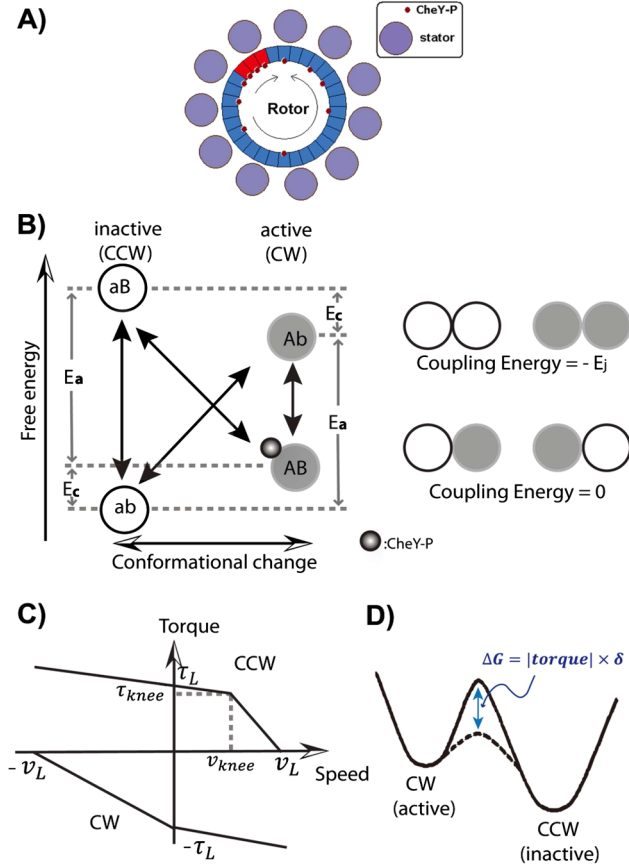
FIG. 1 (color online). Schematic illustration of the BFM torque-generation or switching structure and components of the present model. (A) Schematic top view of the motor. In this figure some RSUs (red) are in the CW state compared to a majority of the inactive RSUs (blue) in the CCW state. (B) Free-energy diagram of the conformational spread model. For simplicity the free-energy difference of conformational change (E_a) between ab and Ab is assumed to be the same as that between AB and aB. Interactions between adjacent RSUs favor pairs with the same conformation by E_j over any unlike pair, independent of CheY-P binding. The relation between the CheY-P binding free energy and the CheY-P concentration is $E_c = -\ln(c/c_{0.5})$. At $c_{0.5}$, there is no bias toward either the CW or the CCW direction. (C) Analytical fitting of the single stator torque-speed curves in the CCW and CW states, where $v_{\rm knee} = 160 \times 2\pi$ rad/s, $\tau_{\rm knee} = 250/4.08 k_B T/$rad, $v_L = 300 \times 2\pi$ rad/s, and $\tau_L = 300/4.08 k_B T/$rad. (D) Stator torque lowers the switching activation energy barrier of contacting RSUs and increases the basic flipping rates $\omega_{\rm flip}$ in the conformational spread model.

Interactions between adjacent RSUs exist with a value $-E_j$ for any like pairs and 0 for any unlike pairs.

(2) With a mean field approximation, the total torque on the rotor is a sum of the torques exerted by individual stators. Each stator functions independently and contributes additively to the overall motor torque. For a given stator, the remaining stators function only as additional effective external torques. For a motor with N stators with a rotation speed v, the force balance relation

gives $\tau_{\rm motor}(v) = \sum_{\alpha=1}^{N} \tau_\alpha(v) = \zeta v$, where $\tau_\alpha(v)$ is the instant torque exerted by stator α, and ζ is the drag coefficient of the external load. A corollary to the approximation is a scaling relation of the steady-state motor torque-speed curves for different N, where $\tau_{\rm motor}(v, N_1)/N_1 = \tau_{\rm motor}(v, N_2)/N_2$. The data points of Ryu *et al* [12] indeed collapse well to a single curve, which supports the validity of the mean field approximation [8]. One can define these normalized curves as the standard torque-speed relationships of a single stator in both CW and CCW directions and fit them analytically with piecewise linear equations [see Fig. 1(c), denoted as $\tau^A(v)$ and $\tau^a(v)$ for later discussions].

(3) Switching rates between the two conformational states of an RSU are affected by the conformation of the neighboring RSUs, as in the conformational spread model $k_{a \to A} = \omega_{\rm flip}(\tau) \exp[0.5\Delta G(a \to A)/k_B T]$, $k_{A \to a} = \omega_{\rm flip}(\tau) \exp[-0.5\Delta G(a \to A)/k_B T]$, where ΔG is the overall free-energy change of the rotor complex associated with the conformation change, and holds one of the following six values: $\pm E_a$ or $\pm(E_a \pm 2E_j)$, and $k_B T$ is the Boltzmann's constant multiplying temperature. We further assume that the instant torque a particular stator imposes on its directly interacting RSU also accelerates the switching rates of the latter, by $\omega_{\rm flip}(\tau) = \omega_0 \exp(|\tau| \times \delta/k_B T)$ [see also Fig. 1(d)], where δ is a scaling factor specifying the strength of torque dependence. Unlike that in [4], here τ is the instant torque an individual stator applies, and it only affects the RSU it contacts. These are essential for our model. See [11] for further discussions on the possible structural explanation of these assumptions.

The CheY-P binding rates are expressed as: $k_{b \to B} = k_{\rm ligand} c/c_{0.5}$, $k_{B \to b} = k_{\rm ligand} \exp(-\Delta G^*(b \to B)/k_B T)$, where c is the concentration of cytoplasmic CheY-P, $c_{0.5}$ is the concentration of CheY-P required for neutral bias, and $\Delta G^*(b \to B)$ is the corresponding CheY-P binding energy, $k_{\rm ligand} = 10$ s^{-1} based on the experimentally determined CheY-P binding rate [5].

(4) Without modeling the torque-generation mechanism in detail (see [11]), which is both computationally expensive and unnecessary for revealing the underlying physics principle, the mean field assumption allows calculating the instant torque of an individual stator directly from the measured BFM torque-speed relations in both CW and CCW directions ($\tau^A(v)$ and $\tau^a(v)$). One can assume that the rotor conformation is in one of the two coherent states under steady rotation. However, during the switch process, the rotor accesses a larger conformational space transiently. There are $2^{26} \sim 6.7 \times 10^7$ possible rotor configurations. The number is large, even taking into account some degeneracy due to symmetry. For a motor under the switching process, supposing at a given time that n_1 of the N (we use $N = 11$ in the following simulations) RSUs that are currently in contact with the N stators are in active conformations, the torque balance of the system gives:

$$n_1 \tau^A(v) + (N - n_1)\tau^a(v) = \zeta v. \qquad (1)$$

The torque required to rotate the external load comes from n_1 stators pushing CW and $(N - n_1)$ stators pushing CCW. From Eq. (1) and the analytically expressed functions $\tau^A(v)$ and $\tau^a(v)$, one can solve the present speed v of the motor and the corresponding instant torque generated by each stator.

We performed stochastic simulations to evolve the motor rotation and switch dynamics simultaneously using the standard Gillespie algorithm [13]. See [11] for more details.

Figure 2(a) shows a typical 30-second switching trace of the time dependence of the rotor angle $\theta(t)$ from the model under a vanishing external load. The model successfully captures the stochastic nature of motor stepping advancement and switching dynamics. Figure 2(b) gives the speed record of the same trace. Motor angular positions are converted to instantaneous speed by dividing the difference between successive angles by the sampling time, 1/3000 s.
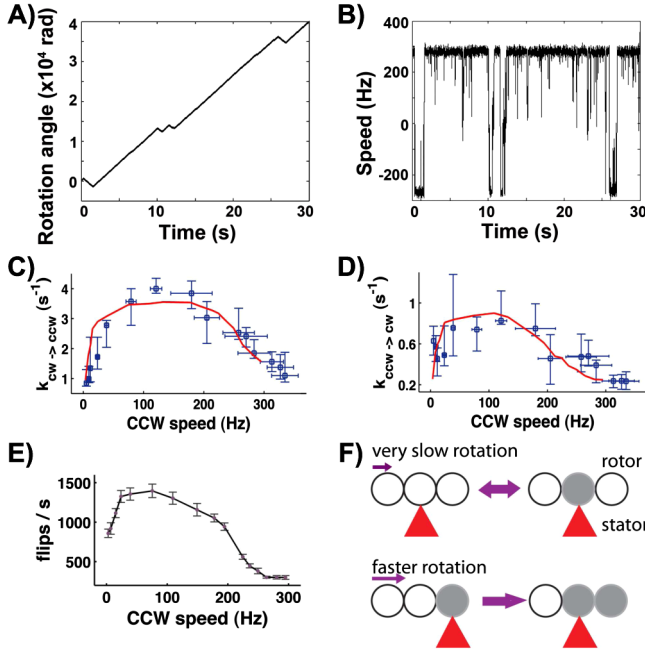

FIG. 2 (color online). Simulation results on the load-switching dynamics. (A) A typical switching angle trace of the BFM (sampled at 3000 Hz) predicted by our model. The simulation is done with model parameters: $E_a = 1k_BT$, $E_j = 4k_BT$, $\omega_0 = 2100$ s^{-1}, $c = 0.9c_{0.5}$, $\delta = 0.04$, drag coefficient of the external load $\zeta = 0.05 k_B T$s/rad^2, as in Ref. [10], and other parameters as in Fig. 1(c). (B) The speed-time trace of the switching angle trace shown in (A). (C–D) Comparison of the experimental (discrete date points) and simulated (solid lines) switching rate–load dependence in both CW and CCW directions. Experimental data points are taken from [4]. (E) Average number of actual conformational changes of a randomly selected RSU on the ring in 1 s. (F) Schematic illustration of coupling between rotation and stator-assisted RSU switching.

To reduce noise, the record of speed vs. time is 40 points moving average filtered before further analysis (same as what has been used experimentally [4]). Consistent with previous studies [10], there are frequent complete switchings between CW and CCW states and incomplete switchings to intermediate speed levels. The switching event between CW and CCW states takes place noninstantaneously, but with a measurable finite switching time.

Figures 2(c) and 2(d) show that the model successfully reproduces the observed nonmonotonic load-switching dependence, and the torque dependence of the switching rates stronger in the CW than that in the CCW direction [3,4]. Our model provides a generic physical explanation of the nonmonotonic feature of the load-switching relationship as follows (for simplicity we focus on the CW → CCW switching): In our model, the frequency of the rotation switching is proportional to the global flipping rate of all the RSUs on the ring, as switching events require a majority of the RSUs to be flipping cooperatively from active to inactive conformation. A key ingredient in our model is that only a few RSUs are aided by torque at any given time. Therefore, at high loads, even though torque facilitation is maximum, this facilitation only involves a few units on which it is locked, which cannot significantly enhance the global switching rate; at low load and thus high speed, the torque helps more RSUs within a unit time, but the facilitation is small, which again cannot significantly increase the global switching rate. Only at an intermediate speed, the torque facilitation is sufficiently strong, and the number of RSUs being helped within a unit time is large, at which point the global switching rate reaches its maximum. Figure 2(e) confirms that at an intermediate speed the average flipping rate of a randomly selected RSU reaches its maximum.

This physical mechanism can also be illustrated by examining the detail of a switching event. The RSU switching dynamics resembles that of the 1-D Ising model. Stochastic fluctuations form small domains of inactive RSUs surrounded by active RSUs. Propagation of the domain wall is the first step to a successful CW → CCW rotor switching. The stators, which interact with only a small number of RSUs, help in the formation of the domain through accelerating the active → inactive RSU conformation conversion. However, for rotations that are too slow, a stator most likely interacts with a single RSU for a long time, causing its conformation to flip back and forth [see Fig. 2(f), top] at a high frequency due to stator facilitation. A domain is formed and destroyed, but it rarely increases in size. On the other hand, for faster rotation, a stator can interact with more RSUs within a given time period, thus helping domain propagation. However, for each individual interacting RSU, stator facilitation is reduced upon increasing rotation speed, making it difficult to create a domain. To substantially increase the probability of successful CW → CCW transitions requires a higher

conformation conversion rate (from stator facilitation) to initialize a domain combined with a timely movement of the ring (from faster rotor rotation) to stabilize and expand the domain [Fig. 2(f), bottom]. Compromise between these two factors makes the maximum switching rate occur at an intermediate motor speed. This mechanism is robust, regardless of most of the model details, such as parameter values, with the only requirements being that the rotor switching takes finite time and the motor torque is a non-increasing function of the rotation speed in both directions. The generality of our results was verified by reproducing the experimental load-switching relationship using a different form of CW state torque-speed relationship, different assumptions on the motor step sizes, and different (E_a, E_j) values in the model, and analyzing the switching dynamics through directly counting the instant CCW protomer number on the rotor ring without the filtering procedure [11].

In summary, we have presented a simple unified mathematical model to explain the load-switching relationship of the bacterial flagellar motor. In our model, (1) torque generation and switching of the BFM have been explicitly modeled and simulated; (2) the conformational spread model, which has successfully reproduced the switching dynamics of the BFM, has been extended to include torque generation and rotor step movement; (3) we invented a new way to calculate the instant torque generated by each stator using experimental data; and (4) we successfully reproduced the experimental data and gave a clear and concise physical picture of the observed phenomena. Van Albada *et al* proposed that a conformational change of the long helical filament contributes to the coupling [14]. However, this elegant model is inconsistent with the conformational spread model and the fact that an *E. coli* flagellar motor with truncated filaments has been used for load-dependence switching measurement.

The significance of the discovery of Berg and coinvestigators is that bacteria like *E. coli* can regulate cell motility using mechanical signaling in addition to other well-studied mechanisms (e.g., chemotaxis). It remains to examine the physiological implications of this observation. Here we provide a few possibilities.

It remains unanswered why all motors in a cell switch almost at the same time [15]. The load-switching relationship provides a cooperative mechanism. A flagellum rotating in an opposite direction to that of other flagella in a bundle experiences an increase in external load from the latter, which helps its motor switch back to the CCW state and then the external hindrance vanishes. Therefore, the majority votes rule. The load-switching relationship may also act as a noise suppressor. Otherwise uncorrelated stochastic switching of the multiple motors should result in more frequent and extended tumbling times than was observed.

In crowded environments (upon cluster forming or under spatial constraint) [16,17], bacteria may sense their surroundings through mechanical force and adjust their moving patterns accordingly. The load-switching dependence may explain the observed variation of the tumbling frequency within a cluster of bacteria [18].

　*keiichi@fbs.osaka-u.ac.jp
　†jxing@vt.edu

[1] H. C. Berg, Annu. Rev. Biochem. **72,** 19 (2003).
[2] Y. Sowa and R. M. Berry, Q. Rev. Biophys. **41,** 103 (2008).
[3] K. A. Fahrner, W. S. Ryu, and H. C. Berg, Nature (London) **423,** 938 (2003).
[4] J. Yuan, K. A. Fahrner, and H. C. Berg, J. Mol. Biol. **390,** 394 (2009).
[5] T. Duke, N. L. Novere, and D. Bray, J. Mol. Biol. **308,** 541 (2001).
[6] J. Xing, F. Bai, R. Berry, and G. Oster, Proc. Natl. Acad. Sci. U.S.A. **103,** 1260 (2006).
[7] G. Meacci and Y. Tu, Proc. Natl. Acad. Sci. U.S.A. **106,** 3746 (2009).
[8] T. Mora, H. Yu, and N. S. Wingreen, Phys. Rev. Lett. **103,** 248102 (2009).
[9] F. Bai, C.-J. Lo, R. M. Berry, and J. Xing, Biophys. J. **96,** 3154 (2009).
[10] F. Bai, R. W. Branch, J. Nicolau, V. Dan, T. Pilizota, B. C. Steel, P. K. Maini, and R. M. Berry, Science **327,** 685 (2010).
[11] See Supplemental Materials at http://link.aps.org/supplemental/10.1103/PhysRevLett.108.178105 for further model details and additional results.
[12] W. Ryu, R. Berry, and H. Berg, Nature (London) **403,** 444 (2000).
[13] D. T. Gillespie, J. Phys. Chem. **81,** 2340 (1977).
[14] S. B. van Albada, S. Tanase-Nicola, and P. R. ten Wolde, Mol. Syst. Biol. **5,** 316 (2009).
[15] L. Turner, R. Zhang, N. C. Darnton, and H. C. Berg, J. Bacteriol. **192,** 3259 (2010).
[16] E. O. Budrene and H. C. Berg, Nature (London) **349,** 630 (1991).
[17] D. E. Woodward, R. Tyson, M. R. Myerscough, J. D. Murray, E. O. Budrene, and H. C. Berg, Biophys. J. **68,** 2181 (1995).
[18] N. Mittal, E. O. Budrene, M. P. Brenner, and A. van Oudenaarden, Proc. Natl. Acad. Sci. U.S.A. **100,** 13259 (2003).